Biosensors and Bioelectronics 78 (2016) 126–131

Contents lists available at ScienceDirect

Biosensors and Bioelectronics

journal homepage: www.elsevier.com/locate/bios

Integration of an optical CMOS sensor with a microfluidic channel allows a sensitive readout for biological assays in point-of-care tests

Bieke Van Dorst [a,*], Monica Brivio [b], Elfried Van Der Sar [c], Marko Blom [b], Simon Reuvekamp [b], Simone Tanzi [b], Roelf Groenhuis [c], Adewole Adojutelegan [c], Erik-Jan Lous [c], Filip Frederix [d], Lieven J. Stuyver [a]

[a] Janssen Diagnostics BVBA, Beerse, Belgium
[b] Micronit Microfluidics, Twente, The Netherlands
[c] NXP Semiconductors, Nijmegen, The Netherlands
[d] NXP Semiconductors, Leuven, Belgium

ARTICLE INFO

Article history:
Received 21 August 2015
Received in revised form
23 October 2015
Accepted 10 November 2015
Available online 11 November 2015

Keywords:
CMOS-based optical sensor
Immunoassays
Microfluidic
Beads

ABSTRACT

In this manuscript, a microfluidic detection module, which allows a sensitive readout of biological assays in point-of-care (POC) tests, is presented. The proposed detection module consists of a microfluidic flow cell with an integrated Complementary Metal–Oxide–Semiconductor (CMOS)-based single photon counting optical sensor. Due to the integrated sensor-based readout, the detection module could be implemented as the core technology in stand-alone POC tests, for use in mobile or rural settings. The performance of the detection module was demonstrated in three assays: a peptide, a protein and an antibody detection assay. The antibody detection assay with readout in the detection module proved to be 7-fold more sensitive that the traditional colorimetric plate-based ELISA. The protein and peptide assay showed a lower limit of detection (LLOD) of 200 fM and 460 fM respectively. Results demonstrate that the sensitivity of the immunoassays is comparable with lab-based immunoassays and at least equal or better than current mainstream POC devices. This sensitive readout holds the potential to develop POC tests, which are able to detect low concentrations of biomarkers. This will broaden the diagnostic capabilities at the clinician's office and at patient's home, where currently only the less sensitive lateral flow and dipstick POC tests are implemented.

1. Introduction

The majority of the diagnostic tests are currently performed in centralized laboratories, following tedious, costly and time consuming procedures that usually require extensive handling. This includes: sample collection from the patient, transfer to the laboratory facility where the sample is analyzed, and sending the results back to the clinician, who then informs the patient. To make this process more efficient, less expensive, and more patient-friendly, there is a high need for point-of-care (POC) tests which enable clinicians or healthcare workers to perform a rapid and easy diagnosis in all clinical settings. Currently available POC tests for use at the clinician's office (including general practitioners) and patient's home are the lateral flow and dipstick tests. These tests are frequently used in cases when the presence or the absence of high abundant biomarkers is relevant for the diagnosis. However, measuring low abundant biomarkers or obtaining quantitative results is not feasible with lateral flow or dipstick tests.

Recently, a considerable effort has been devoted to the development of POC test platforms, which are using lab-on-a-chips (LOC) technologies. These platforms allow to measure or quantify low abundant biomarkers in a fully automated fashion in a relative short time as compared to laboratory-based tests. A disadvantage of these POC test platforms is that they require a readout instrument to perform the tests, which limits the user environment to specialized health departments, since an investment in one or more instruments is required, depending on the application, e.g. DNA/RNA versus peptide/protein/antibody detection. Besides the financial investment, additional requirements on maintenance/calibrations, work space, temperature regulation and electricity might be necessary. This doesn't allow the use of POC test platforms in a mobile or resource limited setting. Recent advancements in nanotechnology, such as disposable biosensors (Janegitz et al., 2014), bring promise to overcome this limitation. By

* Correspondence to: Janssen Diagnostics, Turnhoutseweg 30, 2340 Beerse, Belgium.
E-mail address: bvandors@its.jnj.com (B. Van Dorst).

http://dx.doi.org/10.1016/j.bios.2015.11.027
0956-5663/

integration of biosensors in LOC cartridges (Kumar et al., 2013), an external readout instruments is no longer required. To perform the readout of biological assays on these microfluidic biosensing systems, the microfluidic channel or the biosensor surface is typically functionalized with capture molecules, which bound with the target to be measured. An alternative approach is the use of bead-based microfluidics, in which functionalized microbeads capture target molecules from the sample in a microfluidic channel (Chou et al., 2012; Lim and Zhang, 2007). An important advantage of the bead-based microfluidic approach is the good sensitivity that can be obtained due to the high surface-to-volume ratio, which leads to a more efficient interaction between target and capture molecules. Moreover, the potential to functionalize the beads with different types of capture molecules (antigen, antibody, DNA/RNA, …) allows using one single microfluidic design for a wide range of biological assays.

In this manuscript, it is demonstrated how an optical Complementary Metal–Oxide–Semiconductor (CMOS) sensor can be integrated with a microfluidic channel with a novel beads trapping structure, to allow a sensitive readout of immunoassays. A microfluidic detection module with integrated optical sensor was designed and tested by performing the readout of a peptide, protein and antibody assay.

2. Material and method

2.1. Microfluidic flow cell with integrated optical CMOS sensor

A schematic illustration of the flow cell is given in Fig. 1a. Beads are transported from the inlet reservoir to the beads-trapping region (detailed in Fig. 1b and d) through a 700 μm wide and 8 μm deep microchannel. In the beads-trapping portion of the flow cell, a ridge is designed to leave a 1.5 μm high gap in the flow cell height direction. Fluid can go through the gap while beads are retained and position themselves in the high aspect ratio (width/depth) flow cell forming a well-packed bed above the area interfaced to the sensor (Fig. 1).

The flow cell is made from borosilicate glass in which the channel is etched using a buffered hydrofluoric acid (BHF) solution. The inlet and outlet holes are created by powderblasting. The channel is sealed by direct bonding an unstructured glass wafer onto the etched wafer, forming a so called stack, which is then annealed in an oven. After annealing, gold electrodes are patterned by plasma sputter deposition using a lasercut shadow mask. A 15 nm thick layer of chromium is used to promote adhesion, after which 500 nm of gold is deposited. The stack is then cut into individual flow cells by scribing. Each individual flow cell is integrated with a CMOS-based single photon counting optical sensor (NXP, Netherlands). This CMOS optical sensor has an area of 4.3 mm^2, and includes an on-board temperature sensor, an individual addressable 8×8 pixels array of ultrasensitive photodiodes with a total size of 500 μm × 500 μm, and a digital interface to the outside world. The bonding pads are mounted with conductive glue on the gold electrodes of the flow cell.

The flow cell is mounted in a demo box, which contains the control board to control the readout and pass the readout signal via USB to a computer. To connect the flow cell with the control board, a micro sim connector was used. To obtain a good alignment between the gold electrodes of the flow cell and the micro sim connector and good a fluidic connection towards a vacuum pump at the outlet of the flow cell a Fluidic Connect Pro chip holder (Micronit, Netherlands) in combination with a customized insert was placed on top of the demo boxes.

2.2. Assay methods

2.2.1. HRP IgG detection with a chemiluminescent bead ELISA

In this assay, magnetic beads coated with Protein A were used to detect Immunoglobulin G conjugated with Horseradish Peroxidase (HRP-IgG) (Ortho Clinical Diagnostics, USA). 5 mg of Dynabeads M-270 Epoxy (Life technologies, Belgium) were coated with 50 μg protein A (Thermoscientific, Belgium) according to the instructions for the Dynabeads antibody coupling kit (Life Technologies, Belgium). Before using the protein A coated beads for the detection of HRP-IgG, the beads were blocked with casein, by incubation in 1% casein Phosphate-Buffered Saline (PBS) (Thermoscientific, Belgium) on a roller at room temperature (RT) for 5 min (1 μl of 10 mg beads/ml in 99 μl blocking solution per sample). Afterwards, the beads were separated from the blocking solution with the use of an external magnet and 100 μl of HRP-IgG diluted in 1% casein PBS was added to the beads. The HRP-IgG was incubated for 30 min with the beads on a roller at RT. After this incubation, non-bound IgGs were washed away in three washing

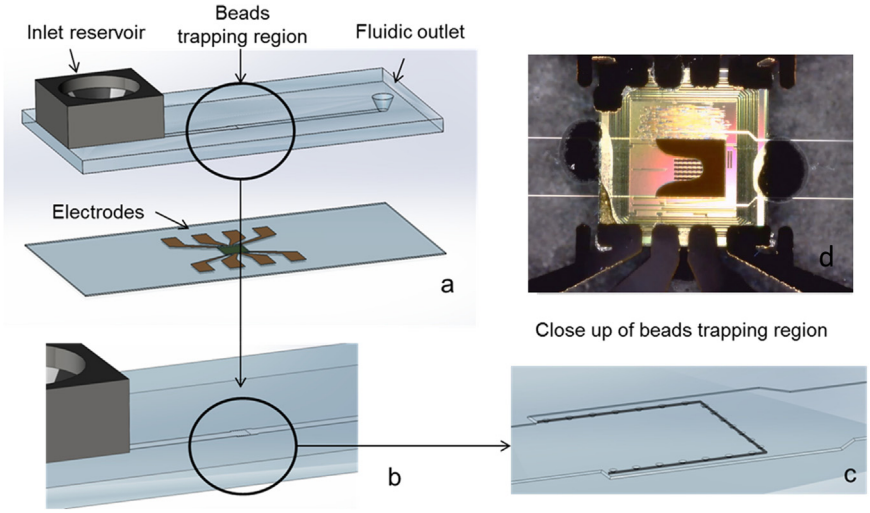

Fig. 1. (a) Schematic representation of the high aspect ratio flow cell assembly with inlet reservoir for beads loading, fluidic outlet and beads trapping region in the top substrate and electrodes patterned on the bottom substrate. (b and c) Close up of the beads trapping region, where pillars fabricated along the ridge with the function keeping the narrow slit of 1.5 μm open are also shown. (d) Photograph of the beads trapping region during loading. Beads with a diameter of 2.8 μm are trapped at the ridge where only a 1.5 μm gap allows fluid to flow through, while beads accumulate in a densely packed configuration.

steps with 200 μl PBST (PBS+0.05% Tween) and one washing step with 50 μl PBS. For each washing step, beads were separated from the liquid with the use of an external magnet and were dissolved in fresh washing buffer. After the last washing step the detection was performed as described in the paragraph readout method.

The chemiluminescent bead assays described below were performed using a identical assay procedure for bead coating, bead blocking and washing.

2.2.2. Amyloid ß42 (Aß42) detection with a chemiluminescent bead ELISA

An amyloid beta 42 (Aß42) specific antibody recognizing the carboxy-terminal end of Aß42 (Department of Neuroscience at Janssen R&D, Belgium) was coated on Dynabeads M-270 Epoxy and blocked. A serial dilution of synthetic Aß42 (Anaspec, USA) was prepared in 0.1% casein. The Aβ42 dilutions were pre-mixed with a detection Aß42-specific antibody conjugated with HRP, but which binds with the amino-terminal end of Aß42 (Department of Neuroscience at Janssen R&D, Belgium). One hundred μl of this Aβ42-detection antibody mixture was incubated with the beads for 30 min on a roller at RT. Non-bound complexes were washed away and the amount of bound complexes was measured.

2.2.3. IFN-gamma-inducible protein 10 (IP-10) detection with a chemiluminescent bead ELISA

Human IP-10 specific capture antibodies (from the IP-10 Human Antibody Pair kit-Life technologies, Belgium) were coated on Dynabeads M-270 Epoxy and blocked with 1% casein. The beads were incubated with a serial dilution of human IP-10 in 1% casein PBS for 1 h at RT. After this incubation, non-bound antibodies were washed away. After the washing steps, the bound IP-10 were detected with the biotin conjugated detection antibody from the IP-10 Human Antibody Pair kit. Therefore, 100 μl of 0.2 μg/ml detection antibody 1% casein PBS was added to each well and incubated for 1 h at RT. After the incubation, non-bound antibodies were washed away. The last incubation step was performed with 100 μl HRP conjugated streptavidin from the IP-10 Human Antibody Pair kit (600 times diluted in 1% casein PBS) for 1 hour at RT. After this last incubation step, non-bound antibodies were washed away and the amount of bound antibodies was measured.

2.2.4. Detection of antibodies specific for John Cunningham virus Polyomavirus capsid protein 1 (JCV VP1) with a chemiluminescent bead ELISA

Recombinant JCV VP1 (Abcam, UK) was coated on Dynabeads M-270 Epoxy and blocked with 1% casein. A serial dilution of a plasma sample obtained from an individual with confirmed JCV infection in 1% casein PBS was incubated with the beads for 1 hour on a roller at RT, non-bound antibodies were washed away, JCV VP1 specific antibodies were detected by an anti-human IgG conjugated with HRP (HRP-IgG).

2.2.5. Detection of JCV VP1 specific antibodies with a colorimetric plate ELISA

A serial dilution of the same plasma sample used for the chemiluminescent bead ELISA with readout on the detection module was measured in colorimetric plate ELISA antibodies for JCV VP1 as described in (Lagatie et al., 2014).

2.3. Readout method

For each sample that was tested, a new flow cell was used. The flow cells were first connected with the demo box and calibrated. During calibration, the photodiodes with a high dark count level were switched off. After the calibration, the dark count or noise level of the sensor, which is the average dark count measured at the different photodiodes that were active after calibration, was measured. Once the dark count was defined, the flow cells were primed from the outlet with PS-atto substrate (Lumigen, USA) by means of a 2 ml syringe. Priming of the flow cells was necessary to avoid air bubbles trapped at the ridge during beads loading (from the inlet).

After the last washing step, the beads were dissolved in 10 μl of PS-atto substrate, and immediately added to the inlet reservoir of the flow cell. By applying vacuum at the outlet, the beads were transported to the sensor area. After 6 min, the flow was stopped by removing the vacuum. To compare luminescent signals measured in different flow cells, a normalized luminescence was calculated with the equation: Normalized Luminescence=(CPS – DC)/DC (CPS= average counts per second of the active photodiodes; DC=dark count).

3. Results and discussion

A detection module is presented in which an optical CMOS sensor is integrated with a bead-based microfluidic channel to allow a sensitive readout of immunoassays. The microfluidic channel design enables to efficiently transport the analyte bound to the beads towards the sensing area where the beads were concentrated above the optical CMOS sensor.

The most commonly used ways to concentrate beads at a specific location in a microfluidic channel are based on physical trapping (Peterson, 2005), which employs physical barriers inside the microfluidic channel, and activation of a magnetic fields to which the beads get attracted (Earhart et al., 2009; Gottheil et al., 2014; Grover and Mathies, 2005; Lien et al., 2007; Zhou et al., 2010).

There are advantages of using a physical trapping over a magnetic trapping:

i) The presence of a barrier, in combination with the geometry of the channel allows the formation of a flat and confined bed of beads, with a limited amount of layers;
ii) beads are loaded and packed in a repeatable way since they are confined by geometrical constrains in a well-defined portion of a channel;
iii) there is no need for external actuators such as magnets.

Due to these advantages, physical trapping was selected for trapping the beads in the detection module described in this paper. Trapping was done by means of a ridge at the bottom of the microfluidic channel, which is designed to leave an opening smaller than the diameter of the beads when the microchannel is sealed with a lid. When the flow is activated, the fluid can flow through the narrow opening, while microbeads are captured and collected in the channel forming a densely packed bed above the sensing area, as shown in Fig. 1. The ridge is U shaped (on three sides) with constant height. First attempts carried out with a single ridge perpendicular to the channel showed that the loading speed decreases significantly with increasing of the amount of beads packed at the ridge, as the already packed beads are contributing to increase the hydraulic resistance of the fluidic network. Therefore ridges were added to the sides, allowing a flow through the side openings. In this configuration, loading of the beads initiates on all of the three sides simultaneously with the three fronts of beads competing on closing in the entire channel area. The width of the side ridges varies along the channel resulting in a higher hydraulic resistance moving away from the perpendicular ridge which allows for a more evenly filled bed of beads with a straight front. The depth of the channel was chosen in such a way that the beads could not be packed with more than

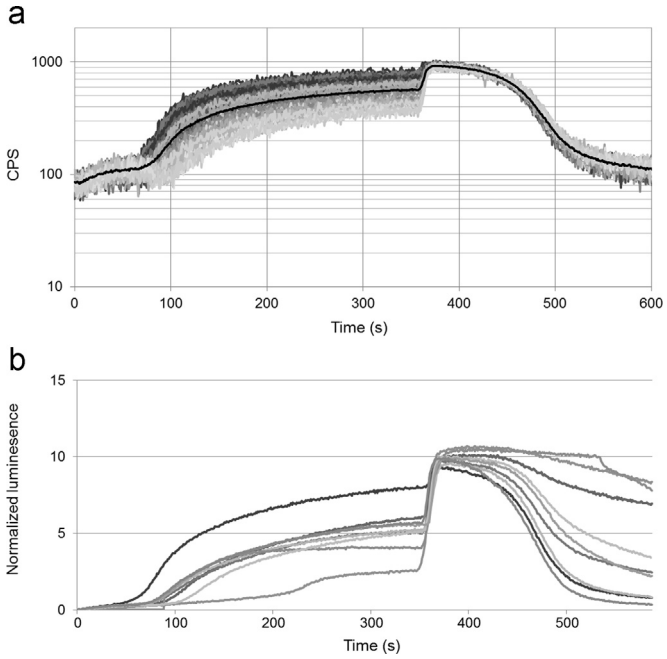

Fig. 2. Difference in Luminescence (a) within the flow cell (at the 64 different photodiodes of the sensor, the black line shows the average of the 64 photodiodes) and (b) between different flow cells (in 9 experiments) in flow condition.

three layers. When multiple layers of beads are formed, the non-transparent beads at the bottom layers would shade the light emitted by the beads in the upper layers. This was observed in preliminary experiments, where a constant amount of 5 amol HRP-IgG coated on different amounts of beads was measured on the CMOS sensor. For these initial experiments the CMOS sensor was not integrated with a flow cell, but the measurements were done with beads directly deposited on the surface of the sensor. These preliminary experiments showed that the signal decreases when more beads layers are formed on the sensor surface (see addendum). In initial bead loading experiments, flow cells with channel shallower than 8 μm were tested in order to obtain less than three beads layers. However, with such channels the beads loading failed before covering the full sensor area.

A first set of experiments using the integrated detection module were performed by measuring a bead-based chemiluminescent reaction in the flow cell under continuous flow conditions. The results of this experiments (Fig. 2) showed large variations in chemiluminescence measured both between different photodiodes within the same flow cell and between flow cells/experiments. The difference in chemiluminescence during continuous flow measurements is probably due to differences in flow rate at different locations in the bead pack, which results from the shape of the ridge (open on three sides, Fig. 1). Although the normalized luminescence under continuous flow conditions shows a very large variation between experiments, it becomes significantly more reproducible at the moment the flow is stopped (Fig. 2b). These results seems to indicate that during flow conditions the substrate molecules do not have enough time to diffuse to the surface of the beads where the reaction with HRP takes place. When the flow is stopped, the substrate molecules are not pushed away by the flow and can diffuse to the beads surfaces where they catalyze the chemiluminescent reaction. The normalized luminescence at the moment the flow is stopped was therefore used as readout signal in all assays reported in this paper.

To define the performance of the stopped flow readout method, the lowest detectable concentration of HRP-IgG was determined. The results reported in Fig. 3 show that the lowest detectable

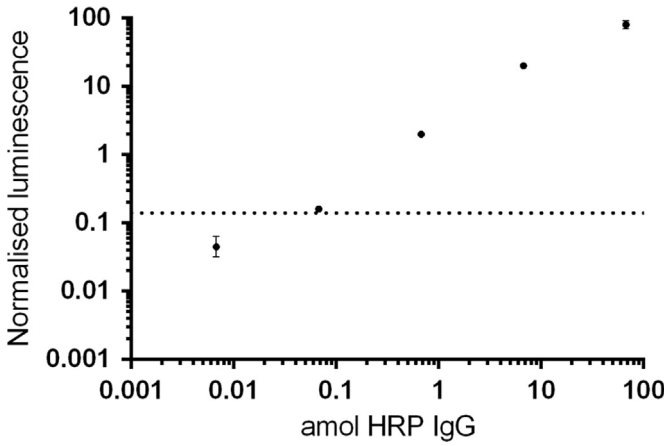

Fig. 3. The normalized luminescence measured on the detection module (Average of $n=3$) for different concentration of HRP-IgG. The error bar shows the SD of the triplicate measurements and the dotted line shows the threshold value, defined by "The average of the blank + 3 × SD" ($n=3$).

concentration of HRP-IgG is 0.0676 amol HRP-IgG (conjugate) (or 676 aM). This means that the detection module with optical CMOS sensor allows the readout of immunoassays with a sensitivity comparable with classical laboratory-based immunoassays. As comparison, for classical laboratory-based immunoassays the lowest detectable concentration of conjugate is in the range of pmol – fmol in case chromogenic substrate are used and in the amol range in case chemiluminescent substrates are used (see http://www.kpl.com/docs/techdocs/KPL%20ELISA%20Technical%20Guide.pdf).

To demonstrate that the detection module can be used for the readout of immunoassays, the performance of three immunoassays,a peptide, a protein and an antibody detection assay, were tested (Fig. 4). As example for a peptide detection assay, an Aß42 assay was used. The results of the measurements of a serial dilution of Aß42 are shown in Fig. 4a. Based on these results the lower limit of detection (LLOD), which is the lowest detectable concentration above the threshold value, with the threshold value defined as "The average of the blank + 3x SD", is defined. The LLOD for the detection of Aß42 is 1 pg/ml or 200 fM (Fig. 4a), which is more sensitive than the commercially available colorimetric plate ELISAs for Aß42 detection (Table 1). Only high sensitive platforms such as Simoa (Quanterix) and V-Plex (Mesoscale) have more sensitive assays available (Table 1). As protein demonstration assay, a cytokine IP-10 was used. The detection of IP-10 showed a LLOD of 4 pg/ml or 460 fM (Fig. 4b), which is in the same range as commercially available colorimetric plate ELISAs and fluorescent bead-based ELISAs (Table 2). Only the high sensitive electrochemiluminescent V-plex (Mesoscale) has a human IP-10 kit available which is more sensitive. Besides the readout of antigen (peptide/proteins) assays, the detection module is capable to perform the readout of antibody assays. To demonstrate this, the amount of JCV VP1 specific antibodies in a serial dilution of a plasma sample obtained from an individual with confirmed JCV infection was determined with both a chemiluminescent bead-based ELISA with readout in the detection module and a classical colorimetric plate-based ELISA. The results in Fig. 4c and d show that the sensitivity of the assay with readout in the developed detection module is 7-fold higher than the colorimetric plate-based ELISA. The lowest detectable dilution of the chemiluminescent bead ELISA with readout in the developed detection module was 82458 times diluted, compared with 12428 times diluted for the colorimetric plate ELISA module (Fig. 4c and d).

The performance of the three demonstrator assays clearly confirms that the detection module can be used for a sensitivity readout of immunoassays. This is better than the traditional lateral

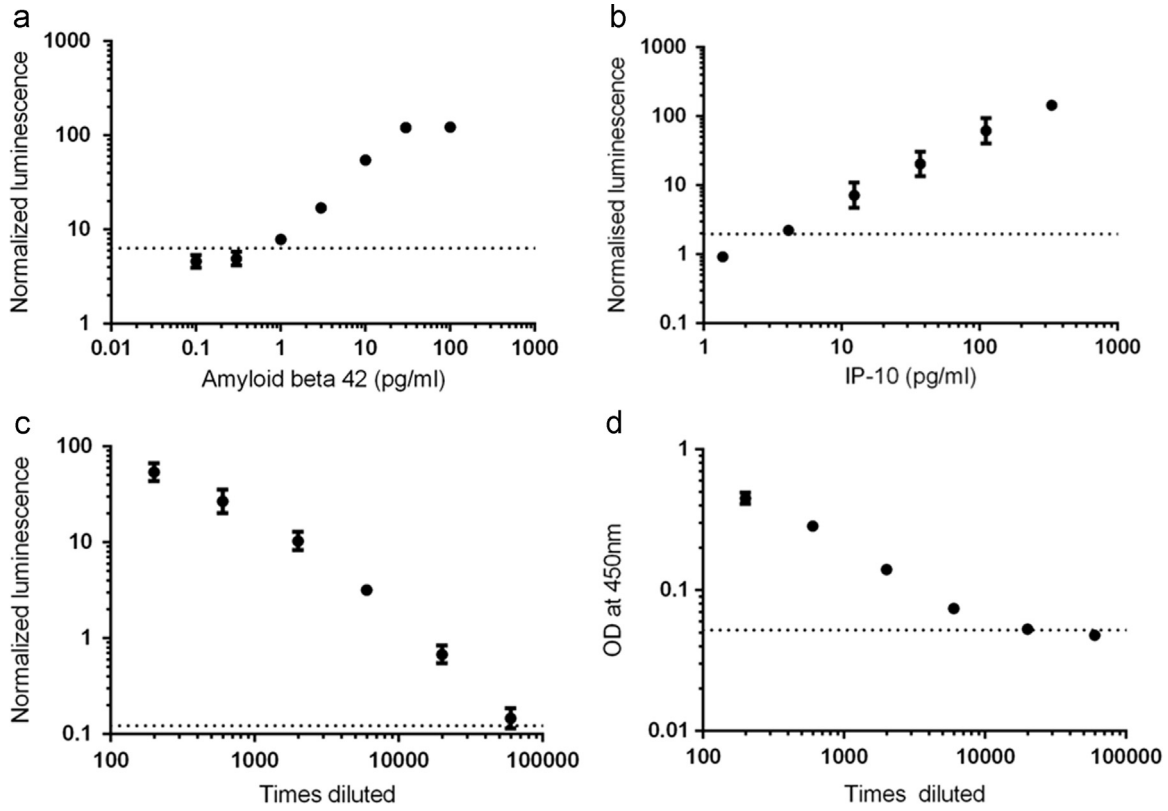

Fig. 4. Results demonstrator assays (a) Detection of amyloid beta 42 by a chemiluminescent bead ELISA with readout in the detection module; (b) Detection of IP-10 by a chemiluminescent bead ELISA with readout in the detection module; (c&d) Detection of JCV VP1 specific antibodies in a diluted plasma sample (c) by a chemiluminescent bead ELISA with readout in the detection module (d) by a colorimetric plate ELISA. The error bars show the SD of the triplicate measurements and the dotted line shows the threshold value, defined by "The average of the blank+3 × SD" ($n=3$).

Table 1
Performance of chemiluminescent bead ELISA with readout in detection module compared with commercially available Aß 42 lab-based assays, according to LLOD reported by manufacturers.

Assay	Type	LLOD (pg/ml)
AlphaLISA (Perkin Elmer)	Amplified luminescent proximity assay	300
Life technologies	Colorimetric	< 10
USCN Lifescience	Colorimetric	4.53
IBL America	Colorimetric	4.03
Sensolyte (Anaspec)	Colorimetric	2
Detection module	**Chemiluminescent**	**1**
V-plex (MSD)	Electrochemiluminescent	0.96
Simoa (Quanterix)	Digital	0.034

Table 2
Performance of chemiluminescent bead ELISA with readout in detection module compared with commercially available IP-10 lab-based assays, according to LLOD reported by manufacturers.

Assay	Type	LLOD (pg/ml)
Luminex human IP10-kit (Biosource/Invitrogen)	Fluorescent bead-based	5
ELISA DuoSet (R&D systems)	Colorimetric	5
ELISA OptEIA (BD biosystems)	Colorimetric	5
Detectionmodule	**Chemiluminescent**	**4**
Luminex Lincoplex (Linco research)	Fluorescent bead-based	3.1
Novex human IP10 ELISA kit (Life technologies)	Colorimetric	2
IP-10 (CXCL10) Human in vitro SimpleStep ELISA (Abcam)	Colorimetric	1.4
V-plex human IP10 kit (Mesoscale)	Electrochemiluminescent	0.37

flow test, using colloid gold nanoparticles as label, with which sensitivities can be obtained of $\pm$10 pM (Gordon and Michel, 2008) and at least equal or better than the more advanced reader-based lateral flow test, using fluorescent or paramagnetic beads ($\pm$0.1 pM) (Sajid et al., 2014) or POC test platforms, such as Minicare (Philips) (1 pM) and iSTAT (Abbot) ($\pm 1-0.1$ pM).

So far the detection module was only used for the readout of traditional bead-based ELISAs, which requires a couple of hours. However, by integration of the ELISA steps in the detection module it could be possible to reduce the time dramatically. Sato et al. (2000) demonstrated with a similar flow cell with packed beads, that the overall assay time of an immunoassay could be reduced from 24 h in the traditional format towards 1 h in the microfluidic flow cell with packed beads, due to the high surface-volume ratio and reduction of the diffusion distance in the flow cell. The possibility to integrated ELISA steps in the detection module and the sensitive readout demonstrated in this manuscript makes the presented detection module valuable as core technology for the development of stand-alone POC tests. This system has several advantages:

i) Existing ELISA assay can be relatively easily transferred to the POC in the microfluidic chip.
ii) The microfluidic chip can be used as a platform for different types of immunoassays. This makes it possible to mass-produce one specific microfluidic chip design at low cost for many diagnostic applications, by using it in combination with differently functionalized beads and reagents.
iii) It improves specificity of testing: a typical problem with clinical immunoassays is the presence of interfering substances (e.g. auto-antibodies or rheumatoid factors (RF), heterophilic antibodies and human anti-mouse antibodies (HAMA)) in whole blood, serum and other human fluid samples, which

may produce abnormally high or false positive immunoassay results (Bolstad et al., 2013). In the heterogeneous ELISA format the interference could be avoided by the use of special blocking agents and washing steps. This is more challenging with the lateral flow format, since washing steps are not possible and preblocking of the strips is not advisable (Posthuma-Trumpie et al., 2009).

4. Conclusion

This manuscript demonstrates the successful integration of a biosensor with a beads-trapping microfluidic flow cell that allows sensitive and quantitative readout of beads-based immunoassays, without the need of an external readout instrument. The detection module described in this paper could be implemented as core technology in the development of stand-alone POC tests, for use in mobile and rural settings. Three demonstrator assays were used as model systems to evaluate the performance of the detection module: a peptide, a protein and an antibody detection assay. The results of this three demonstrator assays showed sensitivities comparable with laboratory-based immunoassays and at least equal or better than current mainstream POC devices. This high sensitivity would allow to develop stand-alone POC tests to measure low concentrations of biomarkers, which can currently only be measured in laboratory-based tests. The availability of such POC tests will broaden the diagnostic capabilities at the clinician's office and at patient's home, where currently only the lateral flow and dipstick POC tests are implemented while low abundant biomarkers can only be detected by sending samples to central laboratories.

Acknowledgments

The authors would like to thank Mark Mercken and Bianca Van Broeck (Department of Neuroscience at Janssen R&D, Belgium) for providing us the amyloid beta 42 (Aß42) specific antibodies.

Addendum

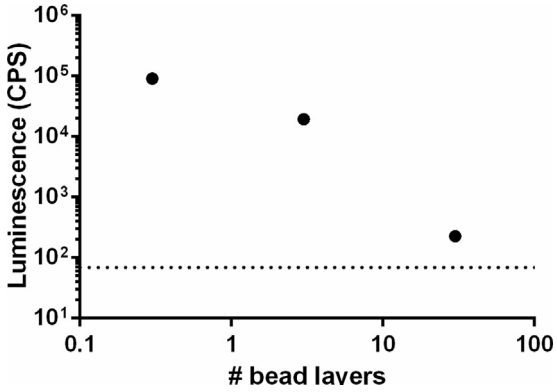

Figure. The luminescence measured by a non-integrated CMOS sensor (Average of n=3) of different layers of beads (estimated based on the number of beads in the detection volume and sensor surface), each one with 5 amol HRP IgG coated on the surface of the beads. The error bars show the SD of the triplicate measurements and the dotted line shows the threshold value, defined by "The average of the blank + 3 x SD" (n=3).

References

Bolstad, N., Warren, D.J., Nustad, K., 2013. Heterophilic antibody interference in immunometric assays. Best practice & research. Clin. Endocrinol. Metab. 27 (5), 647–661.
Chou, J., Wong, J., Christodoulides, N., Floriano, P.N., Sanchez, X., McDevitt, J., 2012. Porous bead-based diagnostic platforms: bridging the gaps in healthcare. Sensors 12 (11), 15467–15499.
Earhart, C.M., Wilson, R.J., White, R.L., Pourmand, N., Wang, S.X., 2009. Microfabricated magnetic sifter for high-throughput and high-gradient magnetic separation. J. Magn. Magn. Mater. 321 (10), 1436–1439.
Gordon, J., Michel, G., 2008. Analytical sensitivity limits for lateral flow immunoassays. Clin. Chem. 54 (7), 1250–1251.
Gottheil, R., Baur, N., Becker, H., Link, G., Maier, D., Schneiderhan-Marra, N., Stelzle, M., 2014. Moving the solid phase: a platform technology for cartridge based sandwich immunoassays. Biomed. Microdevices 16 (1), 163–172.
Grover, W.H., Mathies, R.A., 2005. An integrated microfluidic processor for single nucleotide polymorphism-based DNA computing. Lab. chip 5 (10), 1033–1040.
Janegitz, B.C., Cancino, J., Zucolotto, V., 2014. Disposable biosensors for clinical diagnosis. J. Nanosci. Nanotechnol. 14 (1), 378–389.
Kumar, S., Kumar, S., Ali, M.A., Anand, P., Agrawal, V.V., John, R., Maji, S., Malhotra, B. D., 2013. Microfluidic-integrated biosensors: prospects for point-of-care diagnostics. Biotechnol. J. 8 (11), 1267–1279.
Lagatie, O., Van Loy, T., Tritsmans, L., Stuyver, L.J., 2014. Circulating human microRNAs are not linked to JC polyomavirus serology or urinary viral load in healthy subjects. Virol. J. 11, 41.
Lien, K.Y., Lin, J.L., Liu, C.Y., Lei, H.Y., Lee, G.B., 2007. Purification and enrichment of virus samples utilizing magnetic beads on a microfluidic system. Lab. chip 7 (7), 868–875.
Lim, C.T., Zhang, Y., 2007. Bead-based microfluidic immunoassays: the next generation. Biosens. Bioelectron. 22 (7), 1197–1204.
Peterson, D.S., 2005. Solid supports for micro analytical systems. Lab. chip 5 (2), 132–139.
Posthuma-Trumpie, G.A., Korf, J., van Amerongen, A., 2009. Lateral flow (immuno) assay: its strengths, weaknesses, opportunities and threats. A literature survey. Anal. bioanal. Chem. 393 (2), 569–582.
Sajid, M., Kawde, A., Daud, M., 2014. Designs, formats and applications of lateral flow assay: literature review. J. Saudi Chem. Soc.
Sato, K., Tokeshi, M., Odake, T., Kimura, H., Ooi, T., Nakao, M., Kitamori, T., 2000. Integration of an immunosorbent assay system: analysis of secretory human immunoglobulin A on polystyrene beads in a microchip. Anal. Chem. 72 (6), 1144–1147.
Zhou, Y., Wang, Y., Lin, Q., 2010. A Microfluidic Device for Continuous-Flow Magnetically Controlled Capture and Isolation of Microparticles. Journal of microelectromechanical systems : a joint IEEE and ASME Publication on Microstructures, Microactuators, Microsensors, and Microsystems, 19(4), pp. 743–751.